Journal of Electrical Bioimpedance
www.bioimpedance.net

J Electr Bioimp, vol. 7, pp. 20–27, 2016
Received: 12 Jan 2016, published: 27 May 2016
doi:10.5617/jeb.2657

Simulation of impedance measurements at human forearm within 1 kHz to 2 MHz

Gautam Anand [1,2], Andrew Lowe [1] and Ahmed M. Al-Jumaily [1]

1. *Institute of Biomedical Technologies, Auckland University of Technology, Auckland-1010, New Zealand*
2. *E-mail any correspondence to: gautam.anand@aut.ac.nz*

Abstract
This work presents a simulation analysis of the bioimpedance measurements at the human forearm. The Ansys® High Frequency Structure Simulator (HFSS) has been used to analyze the electrical response of a section of human forearm with three domains of dielectric behavior – fat, muscle and artery (blood). The impedance values were calculated as the ratio of the output voltage at the electrodes to the applied known current (1 mA). A model was developed and was simulated for impedance values obtained within a frequency range of 1 kHz to 2 MHz. The measurements were done at three instances of radial artery diameter. The maximum resistance and reactance values were calculated as 445 Ω and 178.5 Ω, 356 Ω and 138 Ω, and 368 Ω and 144.3 Ω for diameters 2.3 mm, 2.35 mm, and 2.4 mm respectively. The set of impedance values obtained followed the Cole-plot trend. The results obtained were found to be in excellent agreement with the Cole modelling. The set of values obtained at three different diameters reflected the effect of blood flow on impedance values.

Keywords: Bioimpedance, β dispersion, Cole plot, forearm

Introduction

In the last three decades, bioimpedance analysis has become more extensively used to measure clinically important parameters [1]. Non-invasive bioimpedance plethysmography provides waveform information that relates to the distension of blood vessels and can therefore be used for estimating stroke volume [2–5] and cardiac output [6–12]. Bioimpedance offers significant advantages over existing techniques such as ultrasound which requires continuous presence of a trained operator and thermodilution which is an invasive method and cannot readily measure beat-to-beat changes. Electrical impedance measurements at the forearm provide a possible way to characterize hemodynamics, and in particular changes in the amount of blood in the arm as a result of vasodilatation and/or the cardiac cycle.

Although the simulation perspective to bioimpedance plethysmography is a rarity there have been several investigations pertaining to the impedance response at forearm section. Some works [13–16] related to multi-frequency electrical bioimpedance (MF-EBI) for segmental fluid/fat estimation whereas others [17–19] focused on single frequency measurements to evaluate parameters such as Heart Rate (HR) and Pulse Wave Velocity (PWV). Due to a high variability amongst the impedance values obtained from different works, the application dependence of the measurements can be considered a fair statement. The choice of forearm quite obviously owes to the more approximate cylindrical geometry, which makes it easier to construct and analyze. However, more importantly, the blood dynamics of radial artery can be reflected through bioimpedance considering a forearm section. This can provide an insight to the arm tissue behavior along with the individual contribution of different layers (along with blood flow) to the impedance variations. Also, the forearm provides a simpler and justifiable site for PWV measurement

The objective of this work is to simulate the electrical response of a section of human forearm and obtain the values of impedance over a wide frequency range. These simulation results will be compared to the Cole type response. The simu-lation would be performed at three instances of radial artery diameters to mimic the condition of blood flow. The β dispersion region, as identified by Schwan [20] and Cole theory [21] form the basis of this work.

Method

A 3D finite element model of a simplified human forearm was constructed using Ansys® HFSS, which allows simulation of applied electromagnetic fields in the frequency domain.

Our investigation is limited to the β dispersion region as it is in this frequency range (1 kHz to 100 MHz) that the tissues reflect maximum passive cell membrane capacitance and intracellular organelle capacitance effects [22]. The mathematical consideration of bioimpedance theory is governed by Maxwell's equations. For most practical situations, the solution to Maxwell's equations requires a complex matrix approach, which is performed by the finite element modelling platform provided by Ansys® HFSS. Also, the boundary between two dielectrics is automatically specified through Ansys using the defined mesh settings. The forearm was modelled as a structure consisting of three tissue domains – fat, muscle and artery. Even though bone is a major part of the forearm, the overall contribution of bone to the electrical impedance changes is expected to be negligible due to a constant low conductivity over β dispersion frequency range. Hence, bone was not considered to be a part of this model. The fat and muscle regions have been considered as layered, whereas the artery overlaps the domains of both the muscle and fat regions. The tissue domains in the model are therefore not layered. The longitudinal dimension of the section of the arm was taken to be 70 mm, with the fat layer having a thickness of 3 to

6 mm and muscle with a thickness of 10 to 15 mm from the axis. The artery has been modelled to mimic the radial artery blood properties, for which simulation has been performed using three different diameters – 2.3 mm, 2.35 mm, and 2.4 mm as also reported by some previous works [23,24]. The transverse and the longitudinal views of the model are shown in Fig.1 (a) and 1 (b) respectively.

A tetra-polar configuration of electrodes was simulated (also shown in Fig 1). The outer set of electrodes supply the current and the inner pair is used for voltage measurements. The electrodes were realized using cylindrical conductors of copper with a diameter of 2 mm and spacing of 24 mm for the outer pair and 11 mm for the inner pair. Additionally, the outer electrodes were connected through a conducting sheet, over which the direction of current flow was specified for simulation purposes. The frequency dependent dielectric properties for each of the tissue materials have been defined using the database developed by Gabriel [25–28] using the parametric modelling of tissue properties within 10 Hz to 20 GHz (Fig.2). The conductivity and the permittivity values were set for fat, muscle and blood within 1 kHz to 2 MHz.

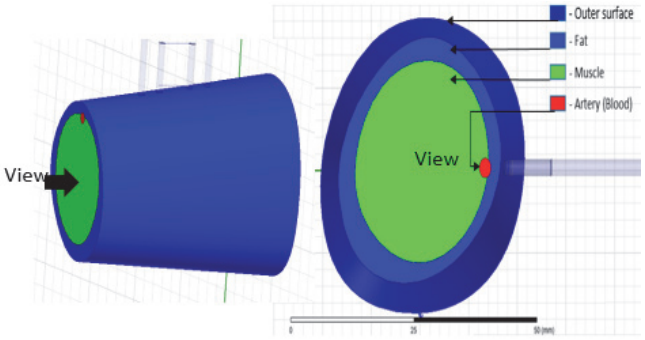

Fig.1 (a): Transverse view of the model

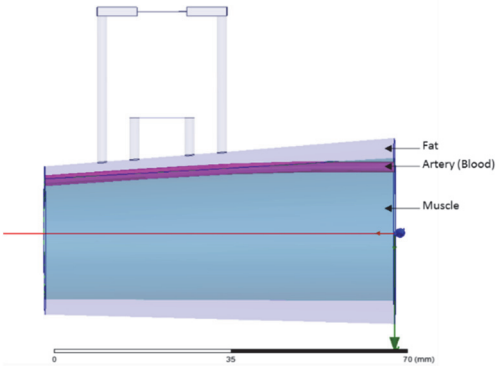

Fig.1 (b): Longitudinal view of the section

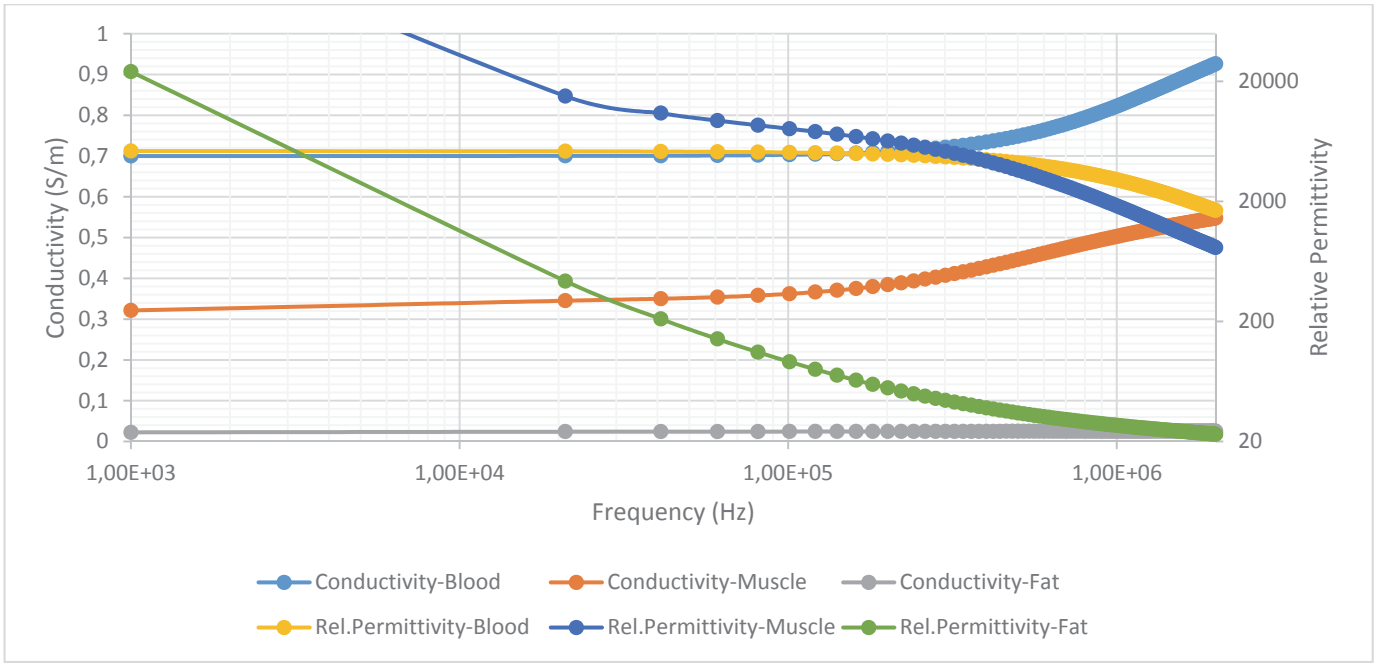

Fig. 2: Conductivity and permittivity values for blood, muscle and fat used in the simulation as compiled by Gabriel [27]

The simulation was performed to determine the value of impedance measured across the electrodes at various frequencies within 1 kHz to 2 MHz. The impedance was calculated as the ratio of measured voltage to the applied current at the corresponding electrodes. IEC 60601 technical standards [29] describe safety of medical equipment and prescribe allowable current ranges. The preferred range is between 10 µA to 1 mA for the frequency range of interest [30] and hence 1 mA was chosen for simulation purposes.

Ansys® was used to automatically mesh with maximum element sizes of 10 mm each for fat and muscle and 5 mm for the artery. Fig.3 – (a), (b), and (c) show the mesh distribution over each of the domains.

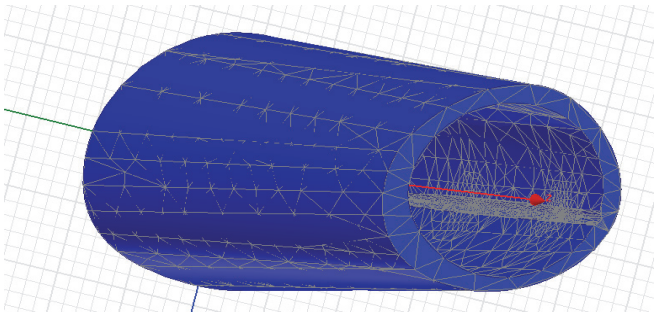

Fig.3 (a): Mesh distribution in the fat layer

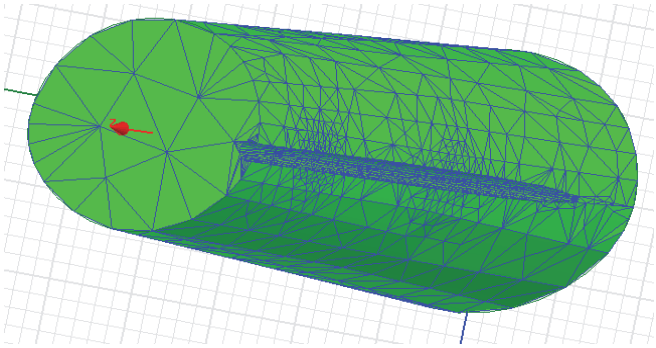

Fig.3 (b): Mesh distribution in the muscle layer with an element size of 10 mm

.

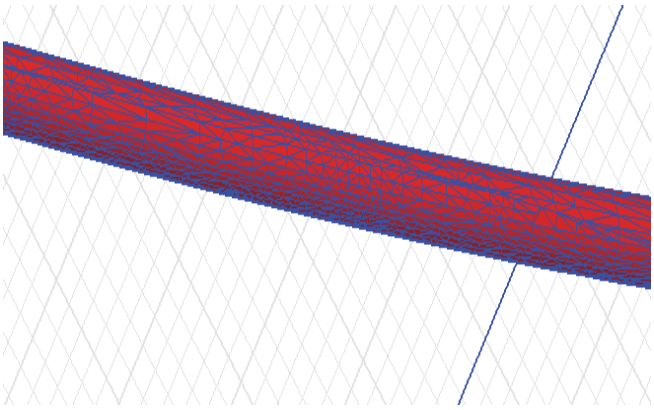

Fig.3 (c): Mesh distribution in the Artery

Simulations were run at frequencies of 1 kHz, 5 kHz, 10 kHz, 50 kHz, 100 kHz, 150 kHz, 200 kHz, 250 kHz, 400 kHz, 500 kHz, 600 kHz, 700 kHz, 800 kHz, 900 kHz, 1 MHz, 1.25 MHz, 1.5 MHz, and 2 MHz. For each of these frequencies, three diameters of the artery were modelled as mentioned previously: 2.3 mm, 2.35 mm, and 2.4 mm.

Results

The simulation was performed to evaluate the dielectric behavior of the compositional properties of fat, muscle and artery in the human forearm. The simulation produced results in the form of electric field distributions (an example shown in Fig. 4 (a) and 4 (b)) throughout the structure at each frequency step, which was used to calculate the voltage drop across the measuring electrodes. The electric field distributions as shown in Fig. 4 (a) and (b) provide a good indication of electric potential gradient throughout the structure volume

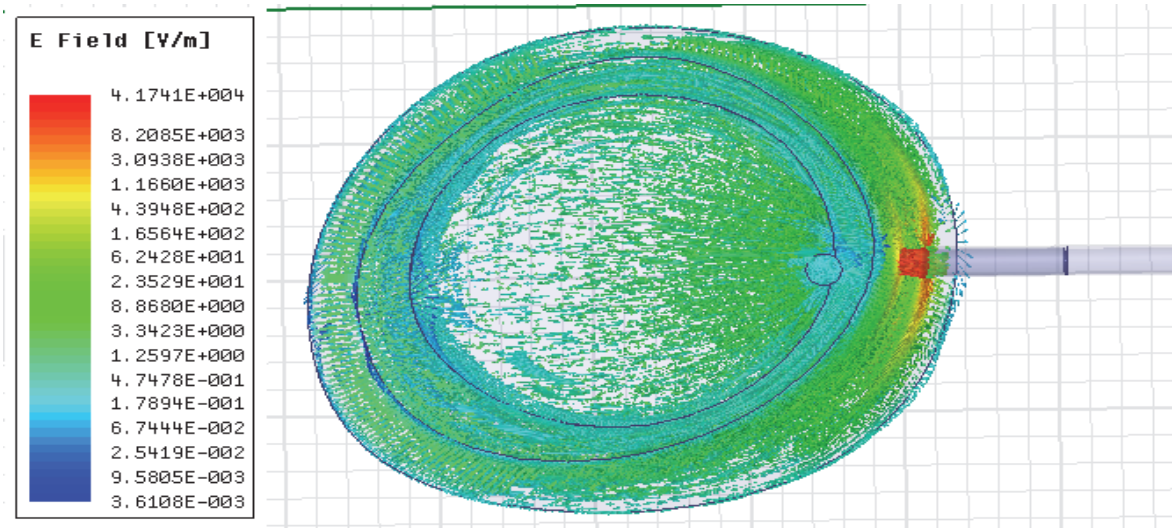

Fig.4 (a): Electric field distribution in the transverse view of the model simulated at 50 kHz for 2.3 mm arterial diameter. The magnitude has been indicated though different color intensities.

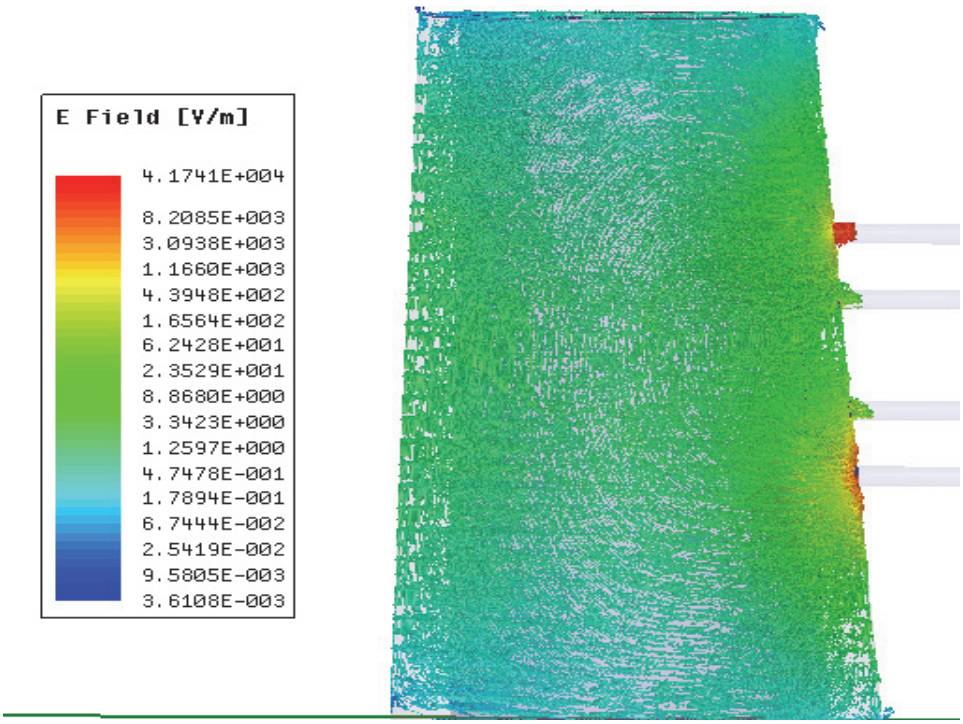

Fig.4 (b): Electric field distribution in the longitudinal view of the model simulated at 50 kHz for 2.3 mm arterial diameter. The magnitude has been indicated though different color intensities.

The voltage was calculated using the line integral of the electric field gradient between the inner electrode pair terminals. The obtained value of the voltage was complex, due to the complex electric field and corresponded to the resistive and reactive behavior of the model. The obtained values have been calculated for impedance (Z) as ratio of measured voltage (V) to current (I) and plotted as a Nyquist plot (as shown in Fig 5) between Re. (Z), i.e. Resistance and Img. (Z), i.e. Reactance for all the frequencies. The three curves correspond to the three diameters of the artery.

Discussion

The electrical behavior of biological tissues can often be effectively represented using the Cole model. The Cole equation describes the frequency dependence of tissue conductivity and permittivity. The results obtained through the simulations agree with the Cole model in the sense of varying resistance and reactance values with frequency. The geometrical interpretation can be seen as Cole plots for all the three diameters. The semi-circular shape of the plot verifies the agreement of the obtained results with Cole modelling (Fig.5). The major portion of the plot follows the Cole plot trend but the values at lower frequencies were found to be divergent.

The maximum resistance and reactance values were calculated as 445 Ω and 178.5 Ω, 356 Ω and 138 Ω, and 368 Ω and 144.3 Ω for diameters 2.3 mm, 2.35 mm, and 2.4 mm respectively. The expected values at the extremities of the Cole plot (R_0 and R_∞) can be found by extrapolating the Cole trend and observing the values at the resistance axis. The above values of the impedance were found within agreeable limits of some previous results such as [31] (which found average value of forearm resistance of 346 Ω) and [32]) (which found mean±standard deviation values of resistance of 319±21.9 Ω and reactance of 30±2.3 Ω for arm at 50 kHz).

The values obtained at lower frequencies do not follow the Cole trend and reflect the minimum values of reactance for each plot. The simulation results at lower frequencies (1 kHz to 200 kHz) were found to be mainly resistive and possessed a different variation of values than the rest of the plot. The high resistance values and corresponding changes with diameters at lower frequencies are a result of significant change in the conductivity due to change in the arterial diameter. Due to the large conductivity of blood, the major change in the impedance occurs as a resistive change due to change in arterial dimension. Hence at lower frequencies, the response is dominantly resistive. The value of maximum reactance for each Cole plot is defined by a characteristic frequency (F_c) which was found to be different for three diameters of the artery.

Although bone as a biological tissue does possess frequency dependent dielectricity, it has a fairly low and constant conductivity over the frequency range of interest. The low variability of conductance makes it a redundant contender for observing impedance changes with pulsating artery. However, it is believed to offer a significant change in overall resistance value while contributing negligibly to the impedance changes with artery diameter and frequency.

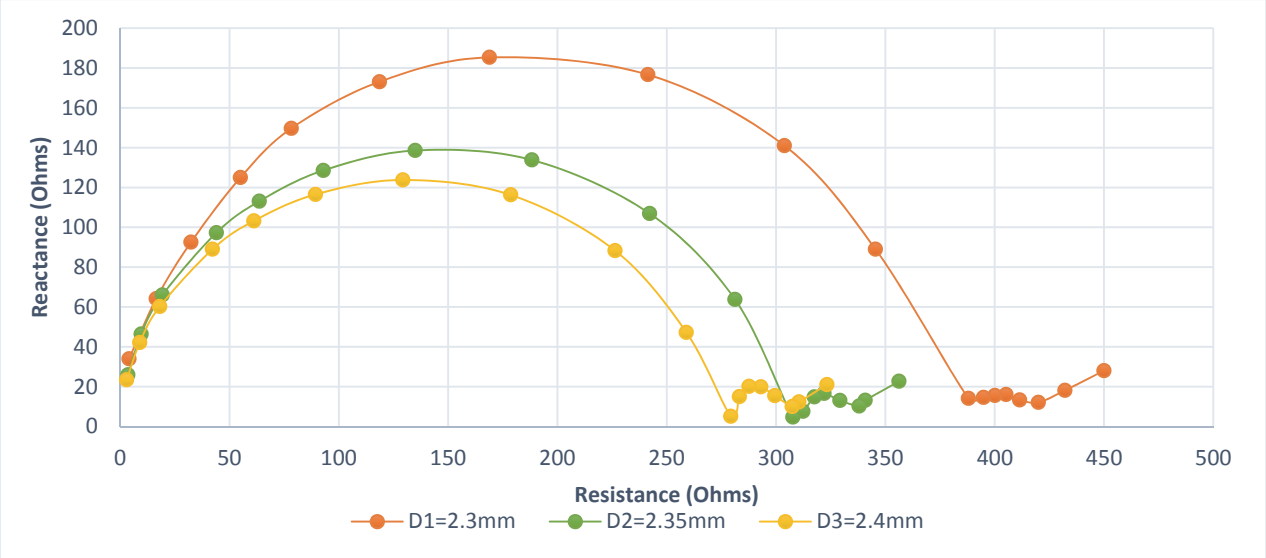

Fig.5: Cole plot of obtained Resistance vs Reactance for three arterial diameters

This work aimed to investigate the overall impedance variations caused by pulsatile flow of blood through the radial artery along with other prominent contributing tissue domains. It might be a good idea to study the overall response with bone included in the model even though its electrical properties do not indicate that it introduces significant changes in the overall behavior in the context of this work.

Although the above simulation model lacks blood flow, the consideration of different arterial diameters partly compensates for the hemodynamic effects. The choice of different arterial diameters complies with the characteristics of arterial system. It was reasonable to assume that the diameter changes uniformly at each wavelength flow of blood, in accordance with long wavelength approximation [33] applied to Moens-Korteweg Equation [34] yielding the expression:

$$c = \sqrt{\frac{Eh}{2r\rho}} \qquad (2)$$

where, E is the arterial elastic modulus, h is the arterial wall thickness, r is the radius and ρ is the blood density. Considering c = f λ, the wavelength (λ) can be calculated using frequency (f) as (72 bpm/60) 1.2 Hz (average) [35]. In this case, the pulse wave velocity (c) can be considered as 8 to 10 m/s (based on results of several works [36–38]) and the maximum fundamental frequency of the blood pressure pulse as 25 Hz [39,40], λ can be evaluated to be 32 to 40 cm which is significantly larger than the dimension of the model. Hence, each wavelength of blood can be assumed 'longer' than the proposed arterial dimensions leading to the consideration of blood flow induced arterial diameter changes. The obtained results with different diameters are important in the sense that they reflect the influence of arterial hemodynamics to the impedance values. The obtained variation in the set of values proves that the composition of tissues along with the hemodynamics serve as important contributors to the overall electrical response. The latter, particularly, has been justified by several works [41–48] analyzing the blood flow effects and contributions to the bioimpedance readings.

The arm structure was enveloped with a radiation boundary and a vacuum region to mimic the prevention of any electromagnetic interference from an outside source. The trade-off between the computing complexity and model efficacy was optimized by selecting the mesh element sizes of 10 and 5 mm for outside layers and artery respectively. Initial simulations with finer mesh sizes produced almost identical results but took longer to converge to a solution. This work neglects the contribution of bone to the overall measurements. Bone is expected to offer higher resistance and capacitance and is predominantly piezoelectric, although dynamic mechanical deformation was not simulated [49].

Also, this study is confined to the compositional properties of blood, fat and muscle tissues and considers dielectric properties to be isotropic. It neglects any dynamic effects, for example, that may cause non-uniform diameter changes along the length of the artery. However, the study provides a useful insight to tissue electrical response through obtained impedance values over the β dispersion frequency range along with changes in impedance variations due to changes in arterial diameter. This can be related to arterial hemodynamics to help estimate the vessel diameter changes through induced impedance variations.

Conclusion

This simulation study aimed at evaluating the impedance values of a section of human forearm Ansys® HFSS was

used to construct and simulate a model consisting of three layers of tissues – fat, muscle and artery and the electrical response was simulated over a frequency range of 1 kHz to 2 MHz.

The effect of blood pulsatile flow has been mimicked and analyzed as the electrical response at three different arterial diameters. This approach provides a simulation perspective to analyze impedance contributions from different tissue layers along with blood dynamics. The obtained results clearly assert a good capability of the setup to be quite sensitive towards diameter changes. This may aid future works in investigating the electrical variations due to pulsating artery. The study highlights a basic understanding of the frequency dependent electrical behavior of human forearm tissues and presents an efficient simulation tool to analyze the effects and individual contributions of different tissues to the bioimpedance measurements.

References

1. Grimnes S, Martinsen ØG. Bioimpedance. Wiley Encyclopedia of Biomedical Engineering [Internet]. John Wiley & Sons, Inc.; 2006. Available from: http://dx.doi.org/10.1002/9780471740360.ebs0128
2. Secher NJ, Thomsen A, Arnsbo P. Measurement of rapid changes in cardiac stroke volume. An evaluation of the impedance cardiography method. Acta Anaesthesiol Scand. 1977;21(5):353–8. http://dx.doi.org/10.1111/j.1399-6576.1977.tb01231.x
3. Quail AW, Traugott FM, Porges WL, White SW. Thoracic resistivity for stroke volume calculation in impedance cardiography. J Appl Physiol. 1981 Jan 1;50(1):191–5.
4. Gratze G, Fortin J, Holler A, Grasenick K, Pfurtscheller G, Wach P, Schönegger J, Kotanko P, Skrabal F. A software package for non-invasive, real-time beat-to-beat monitoring of stroke volume, blood pressure, total peripheral resistance and for assessment of autonomic function. Comput Biol Med. 1998;28(2):121–42. http://dx.doi.org/10.1016/S0010-4825(98)00005-5
5. Henry IC, Bernstein DP, Banet MJ. Stroke volume obtained from the brachial artery using transbrachial electrical bioimpedance velocimetry. 2012 Annual International Conference of the IEEE Engineering in Medicine and Biology Society (EMBC). 2012. p. 142–5.
6. Enghoff E, Lovheim O. A comparison between the transthoracic electrical impedance method and the direct Fick and the dye dilution methods for cardiac output measurements in man. Scand J Clin Lab Invest. 1979;39(6):585–90. http://dx.doi.org/10.3109/00365517909108837
7. Edmunds AT, Godfrey S, Tooley M. Cardiac output measured by transthoracic impedance cardiography at rest, during exercise and at various lung volumes. Clin Sci. 1982;63(2):107–13. http://dx.doi.org/10.1042/cs0630107
8. Judy WV, Powner DJ, Parr K, Demeter R, Bates C, Marshall S. Comparison of electrical impedance and thermal dilution measured cardiac output in the critical care setting. Crit Care Med. 1985;13(4):305. http://dx.doi.org/10.1097/00003246-198504000-00068
9. Appel PL, Kram HB, MackAbee J, Fleming AW, Shoemaker WC. Comparison of measurements of cardiac output by bioimpedance and thermodilution in severely ill surgical patients. Crit Care Med. 1986;14(11):933–5. http://dx.doi.org/10.1097/00003246-198611000-00004
10. Gotshall RW, Wood VC, Miles DS. Comparison of two impedance cardiographic techniques for measuring cardiac output. Ann Biomed Eng. 1989;17(5):495–505. http://dx.doi.org/10.1007/BF02368069
11. Bloch KE, Russi EW. Comparison of impedance cardiography to invasive techniques for measurement of cardiac output. Am J Cardiol. 1997;79(6):846–846.
12. Keren H, Burkhoff D, Squara P. Evaluation of a noninvasive continuous cardiac output monitoring system based on thoracic bioreactance. Am J Physiol - Heart Circ Physiol. 2007 Jul 1;293(1):H583–9. http://dx.doi.org/10.1152/ajpheart.00195.2007
13. Pietrobelli A, Nu-ez C, Zingaretti G, Battistini N, Morini P, Wang ZM, Yasumura S, Heymsfield SB. Assessment by bioimpedance of forearm cell mass: a new approach to calibration. Eur J Clin Nutr. 2002 Aug;56(8):723–8. http://dx.doi.org/10.1038/sj.ejcn.1601384
14. Ohmine Y, Morimoto T, Kinouchi Y, Iritani T, Takeuchi M, Haku M, Nishitani H. Basic study of new diagnostic modality according to non-invasive measurement of the electrical conductivity of tissues. J Med Invest. 2004;51(3-4):218–25. http://dx.doi.org/10.2152/jmi.51.218
15. Raja MK. Changes in tissue water content measured with multiple-frequency bioimpedance and metabolism measured with 31P-MRS during progressive forearm exercise. J Appl Physiol. 2006 Oct 1;101(4):1070–5. http://dx.doi.org/10.1152/japplphysiol.01322.2005
16. Simini F, Bertemes-Filho P. II Latin American Conference on Bioimpedance: 2nd CLABIO,Montevideo,September 30 - October 02, 2015. Springer; 2015. 98 p.
17. Metshein M, Parve T. Towards a Wearable Device for Capacitive Monitoring of Electrical Bioimpedance of Human Body. [cited 2016 Jan 11]; Available from: http://www.isbem.org/conf/2015/proc/03.pdf
18. Nahrstaedt H, Schauer T. A bioimpedance measurement device for sensing force and position in neuroprosthetic systems. 4th European Conference of the International Federation for Medical and Biological Engineering [Internet]. Springer; 2009 [cited 2016 Jan 11]. p. 1642–5. Available from: http://link.springer.com/chapter/10.1007/978-3-540-89208-3_390 http://dx.doi.org/10.1007/978-3-540-89208-3_390

19. Matejkova M, Vondra V, Halamek J, Soukup L, Plesinger F, Viscor I, Jurak P. Measurement of pulse wave velocity during valsalva and mueller maneuvers by whole body impedance monitor. Computing in Cardiology Conference (CinC), 2014 [Internet]. IEEE; 2014 [cited 2016 Jan 11]. p. 1117–20. Available from: http://ieeexplore.ieee.org/xpls/abs_all.jsp?arnumber=7043243

20. Schwan HP. Electrical properties of tissue and cell suspensions. Adv Biol Med Phys. 1957;5:147. http://dx.doi.org/10.1016/B978-1-4832-3111-2.50008-0

21. Cole KS, Cole RH. Dispersion and absorption in dielectrics I. Alternating current characteristics. J Chem Phys. 1941;9(4):341–51. http://dx.doi.org/10.1063/1.1750906

22. Grimnes S, Martinsen OG. Bioimpedance and Bioelectricity Basics. Academic Press; 2014. 585 p.

23. Mooser V, Etienne J-D, Farine P-A, Monney P, Perret F, Cecchini M, Gagnebin E, Bornoz C, Tardy Y, Arditi M, Meister J-J, Leuenberger C-E, Saurer E, Mooser E, Waeber B, Brunner HR. Non-invasive measurement of internal diameter of peripheral arteries during the cardiac cycle. J Hypertens. 1988 Dec;6(4):S179-S181. http://dx.doi.org/10.1097/00004872-198812040-00053

24. Trazzi S, Omboni S, Santucciu C, Parati G, Mancia G. Variability in arterial diameter and compliance: compliance modulation reserve. J Hypertens. 1992 Aug;10(6):S41-S43. http://dx.doi.org/10.1097/00004872-199208001-00011

25. Gabriel C. Compilation of the Dielectric Properties of Body Tissues at RF and Microwave Frequencies. [Internet]. DTIC Document; 1996 [cited 2015 Nov 29]. Available from: http://oai.dtic.mil/oai/oai?verb=getRecord&metadataPrefix=html&identifier=ADA309764

26. Gabriel C, Gabriel S, Corthout E. The dielectric properties of biological tissues: I. Literature survey. Phys Med Biol. 1996;41(11):2231. http://dx.doi.org/10.1088/0031-9155/41/11/001

27. Gabriel S, Lau RW, Gabriel C. The dielectric properties of biological tissues: II. Measurements in the frequency range 10 Hz to 20 GHz. Phys Med Biol. 1996 Nov 1;41(11):2251–69. http://dx.doi.org/10.1088/0031-9155/41/11/002

28. Gabriel S, Lau RW, Gabriel C. The dielectric properties of biological tissues: III. Parametric models for the dielectric spectrum of tissues. Phys Med Biol. 1996;41(11):2271. http://dx.doi.org/10.1088/0031-9155/41/11/003

29. IEC 60601. Wikipedia, the free encyclopedia [Internet]. 2015 [cited 2015 Dec 5]. Available from: https://en.wikipedia.org/w/index.php?title=IEC_60601&oldid=685994304

30. Olson WH. Electrical safety. Med Instrum Appl Des [Internet]. 1978 [cited 2015 Dec 5]; Available from: https://eva.fing.edu.uy/pluginfile.php/68296/mod_resource/content/1/c14.pdf

31. Frydrysiak M, Zięba J, Tęsiorowski L, Tokarska M. Textronic system to muscle electrostimulation. PES. 2012;149:0–41.

32. Savegnago M, Rodrigues de O F, Iraci R, Jordão J, Afonso A, García Ch P, others. Determinación de composición corporal mediante análisis de impedancia segmentada: consideraciones y aplicaciones prácticas. Rev Chil Nutr. 2010;37(3):262–8. http://dx.doi.org/10.4067/S0717-75182010000300001

33. Alastruey J, Parker KH, Sherwin SJ. Arterial pulse wave haemodynamics. Anderson 11th International Conference on Pressure Surges [Internet]. 2012 [cited 2015 Dec 6]. p. 401–42. Available from: http://wwwf.imperial.ac.uk/ssherw/spectralhp/papers/PulseSurges_2012.pdf

34. Moens–Korteweg equation. Wikipedia, the free encyclopedia [Internet]. 2015 [cited 2015 Dec 6]. Available from: https://en.wikipedia.org/wiki/Moens%E2%80%93Korteweg_equation

35. Li JK-J. Comparative Cardiovascular Dynamics of Mammals. CRC Press; 1995. 176 p.

36. Asmar R, Benetos A, Topouchian J, Laurent P, Pannier B, Brisac A-M, Target R, Levy BI. Assessment of Arterial Distensibility by Automatic Pulse Wave Velocity Measurement Validation and Clinical Application Studies. Hypertension. 1995 Sep 1;26(3):485–90. http://dx.doi.org/10.1161/01.HYP.26.3.485

37. Wilkinson IB, Fuchs SA, Jansen IM, Spratt JC, Murray GD, Cockcroft JR, Webb DJ. Reproducibility of pulse wave velocity and augmentation index measured by pulse wave analysis. J Hypertens. 1998;16(12):2079–84. http://dx.doi.org/10.1097/00004872-199816121-00033

38. Salvi P, Lio G, Labat C, Ricci E, Pannier B, Benetos A. Validation of a new non-invasive portable tonometer for determining arterial pressure wave and pulse wave velocity: the PulsePen device. J Hypertens. 2004;22(12):2285–93. http://dx.doi.org/10.1097/00004872-200412000-00010

39. Brans YW, Hay WW. Physiological Monitoring and Instrument Diagnosis in Perinatal and Neonatal Medicine. CUP Archive; 1995. 428 p.

40. Pauca AL. The second peak of the radial artery pressure wave represents aortic systolic pressure in hypertensive and elderly patients. Br J Anaesth. 2004 Mar 19;92(5):651–7. http://dx.doi.org/10.1093/bja/aeh121

41. Sigman E, Kolin A, Katz L, Jochim K. Effect of motion on the electrical conductivity of the blood. Am J Physiol Content. 1937;118(4):708–19.

42. Edgerton RH. Conductivity of sheared suspensions of ellipsoidal particles with application to blood flow. Biomed Eng IEEE Trans On. 1974;(1):33–43.

43. Dellimore JW, Gosling RG. Change in blood conductivity with flow rate. Med Biol Eng. 1975 Nov 1;13(6):904–13. http://dx.doi.org/10.1007/BF02478096

44. Sakamoto K, Kanai H. Electrical Characteristics of Flowing Blood. IEEE Trans Biomed Eng. 1979 Dec;BME-26(12):686–95. http://dx.doi.org/10.1109/TBME.1979.326459

45. Hause LL, Gayon F., Aleksza ME. Impedance measurements during simulated blood flow. Engineering in Medicine and Biology Society, 1989 Images of the Twenty-First Century, Proceedings of the Annual International Conference of the IEEE Engineering in. 1989. Vol. 4. p. 1232. http://dx.doi.org/10.1109/iembs.1989.96169

46. Shmulewitz A, Wallace AA. Apparatus and methods of bioelectrical impedance analysis of blood flow. US6095987 A, 2000.

47. Gaw RL, Cornish BH, Thomas BJ. The Electrical Impedance of Pulsatile Blood Flowing Through Rigid Tubes: A Theoretical Investigation. IEEE Trans Biomed Eng. 2008 Feb;55(2):721–7. http://dx.doi.org/10.1109/TBME.2007.903531

48. Corciova C, Ciorap R, Zaharia D, Matei D. On using impedance plethysmography for estimation of blood flow. 2011 IEEE International Workshop on Medical Measurements and Applications Proceedings (MeMeA). 2011. p. 84–7.

49. Reddy GN, Saha S. Electrical and dielectric properties of wet bone as a function of frequency. Biomed Eng IEEE Trans On. 1984;(3):296–303